

ORGANIC CHEMISTRY

FRONTIERS



CHINESE
CHEMICAL
SOCIETY



ROYAL SOCIETY
OF CHEMISTRY

rsc.li/frontiers-organic

RESEARCH ARTICLE

[View Article Online](#)
[View Journal](#) | [View Issue](#)



Cite this: *Org. Chem. Front.*, 2021, **8**, 4678

Received 1st May 2021,
 Accepted 18th June 2021
 DOI: 10.1039/d1qo00686j
rsc.li/frontiers-organic

Aryl carbazole-based macrocycles: synthesis, their remarkably stable radical cations and host–guest complexation with fullerenes[†]

Lijun Mao, Manfei Zhou, Yan-Fei Niu, Xiao-Li Zhao and Xueliang Shi *

A series of fully conjugated macrocycles **M_n** ($n = 4–7$) consisting of *N*-(3,5-di-*tert*-butyl-4-methoxyphenyl) substituted carbazole (**Cz-Ar**) were successfully synthesized. The aryl carbazole and macrocycle **M₄** can be readily oxidized and the corresponding radical cation species were found to be highly stable. Moreover, macrocycle **M₅** was found to form 1:1 stoichiometric complexes with fullerenes **C₆₀** and **C₇₀** with association constants as high as $(8.38 \pm 0.33) \times 10^4 \text{ M}^{-1}$ and $(7.64 \pm 0.26) \times 10^4 \text{ M}^{-1}$, respectively.

Carbazole is one of the most commonly used building blocks for a wide range of organic electronic applications such as organic solar cells (OSCs), organic light-emitting diodes (OLEDs), organic field-effect transistors (OFETs) and so on.¹ The inherent electron-donating ability of carbazole facilitates its hole-injection and transport, which are very conducive to realizing the excellent optoelectronic properties of carbazole-based organic functional materials, such as their good conductivity and high photoluminescence efficiency.² Generally, the hole-injection process of the carbazole-based materials is often accompanied by the formation of a carbazole radical cation species (sometimes called a polaron), which has been intensively investigated in the fields of OSCs and OLEDs. However, the precise structural characterization of the carbazole radical cation species is relatively rare, especially the lack of the X-ray diffraction structure.³ This is largely due to the fact that most carbazole radical cation species are highly reactive and readily undergo dimerization and polymerization, and therefore usually unstable.⁴

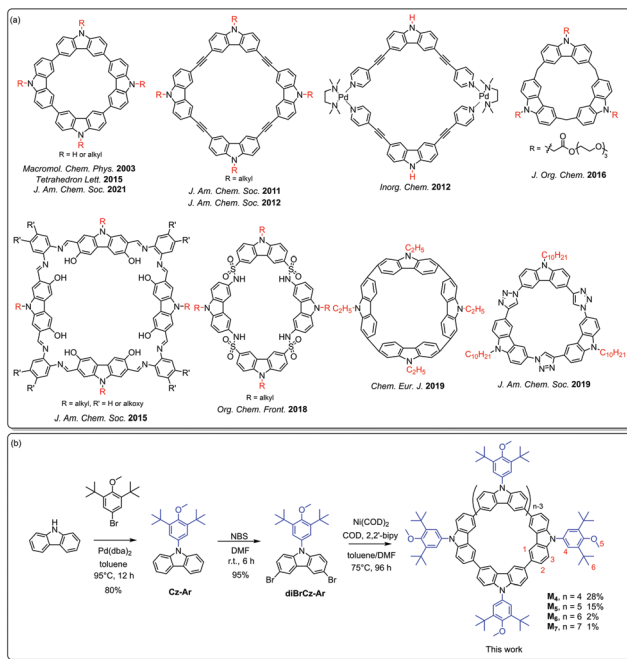
Supramolecular macrocycles containing a variety of building blocks such as phenol,⁵ pyrrole,⁶ glycoluril,⁷ *para*-dialkoxybenzene⁸ and so on⁹ are well known as guest receptors in supramolecular host–guest chemistry. Carbazole, one of the most common building blocks in organic synthesis,^{1,2} has also been widely used as a versatile building unit in supramolecular chemistry. Carbazole has several distinct merits such as its facile synthesis and easy modification, its structural rigidity

with a well-defined molecular geometry, and its intriguing redox-active and luminescence properties, which make it ideal for the synthesis of a number of shape-persistent macrocycles with unique structures, novel properties, and potential applications. During the past decades, a variety of carbazole-based macrocyclic systems, including tricarbazole triazolophanes,¹⁰ carbazole-based Schiff base macrocycles,¹¹ carbazolophanes,¹² calix[n]carbazole,¹³ conjugated polycarbazoles,¹⁴ cyclo[4]carbazole,¹⁵ carbazole–ethynylene macrocycles,¹⁶ azacalix[2]arene[2]carbazoles,¹⁷ carbazole-based metallacycles¹⁸ and so on,¹⁹ have been successfully developed, and some of them have been shown to have potential applications in molecular recognition, catalysis, and supramolecular self-assembly (Scheme 1a). Notably, the nitrogen atom of the carbazole unit in most of the documented carbazole-based macrocycles is substituted with the alkyl side-chain, while aryl carbazole based macrocycles still remain unexplored. We infer that the substitution of the aryl group on the nitrogen atom of carbazole would have a pronounced effect on the properties of the resultant aryl carbazole based macrocycles.

In this work, we have designed and synthesized a series of fully conjugated macrocycles **M_n** ($n = 4–7$) consisting of *N*-(3,5-di-*tert*-butyl-4-methoxyphenyl) substituted carbazole (**Cz-Ar**) (Scheme 1b). The introduction of the 3,5-di-*tert*-butyl-4-methoxyphenyl group at the nitrogen atom of the carbazole reduced the ionization energy and enhanced the stability of the carbazole radical cation. Consequently, a mixed-valence radical cation of $(\text{diBrCz-Ar})_2^{+}$ was successfully isolated in a stable single crystal form for the first time. The stability of the carbazole radical cation was further enhanced within the framework of **M₄** because of the efficient spin delocalization through the enlarged macrocyclic π -system. Moreover, the interesting host–guest interactions between these aryl carbazole-based macrocycles and fullerenes were also investigated.

Shanghai Key Laboratory of Green Chemistry and Chemical Processes, School of Chemistry and Molecular Engineering, East China Normal University, Shanghai 200062, P. R. China. E-mail: xlshi@chem.ecnu.edu.cn

[†] Electronic supplementary information (ESI) available. CCDC 2071725 (**diBrCz-Ar**)₂(DDQ), 2071727 (**M₄**), 2071729 (**M₅**) and 2073892 (**diBrCz-Ar**). For ESI and crystallographic data in CIF or other electronic format see DOI: 10.1039/d1qo00686j



Scheme 1 (a) Chemical structures of some representative carbazole-based macrocycles in the literature. (b) Synthesis of the macrocycles **M_n** (n = 4–7) consisting of *N*-(3,5-di-*tert*-butyl-4-methoxyphenyl) substituted carbazole (**Cz-Ar**).

Results and discussion

As shown in Scheme 1b, *N*-(3,5-di-*tert*-butyl-4-methoxyphenyl) substituted carbazole (**Cz-Ar**) was prepared through the Buchwald–Hartwig amination of carbazole with 5-bromo-1,3-di-*tert*-butyl-2-methoxybenzene in 80% yield. Bromination of **Cz-Ar** using *N*-bromosuccinimide in a dichloromethane (DCM) solution gave *N*-aryl-3,6-dibromocarbazole (**diBrCz-Ar**) in 95% yield. Subsequently, the $\text{Ni}(\text{cod})_2$ /bpy-mediated homocoupling of **diBrCz-Ar** afforded a series of macrocycles **M_n** (n = 4–7),¹⁵ which were successfully separated and purified by preparative gel permeation chromatography (GPC), using DCM as an eluent. The tetramer **M₄**, pentamer **M₅**, hexamer **M₆** and heptamer **M₇** were obtained in 28%, 15%, 2% and 1% yields, respectively, and they exhibited excellent solubility in common organic solvents. The modest yields of **M₄** and **M₅** were attributed to the bulky aryl substituent which significantly enhanced their solubilities. In contrast, the Yamamoto homocoupling of *N*-butyl-3,6-dibromocarbazole (**diBrCz-C4**) gave the main product of the tetramer **C4-M₄**, while other bigger analogues including the pentamer were hardly isolated due to their extremely low yields, which are mostly caused by their low solubilities (Fig. S1†).¹⁵ The structures of **Cz-Ar**, **diBrCz-Ar**, and macrocycles **M_n** were thoroughly characterized by ¹H and ¹³C NMR and HR-MS measurements (see the ESI†).

Single crystals suitable for X-ray crystallographic analysis were obtained for **M₄** and **M₅** by slow diffusion of methanol into chloroform solution (Fig. 1), which unambiguously confirmed their macrocyclic structures. Tetramer **M₄** adopted a

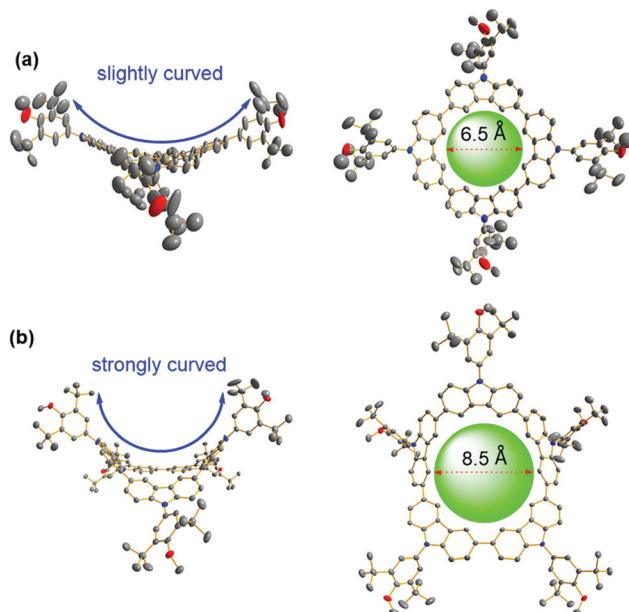


Fig. 1 Crystal structures of tetramer **M₄** (a) and pentamer **M₅** (b). Ellipsoids are represented with 50% probability. Hydrogen atoms and the solvent are omitted for clarity.

slightly curved conformation in the crystalline state (Fig. 1a), in contrast to the nearly planar structure of its *N*-alkyl substituted analogue **C4-M₄**.^{15c} Macrocycle **M₅** further twisted and adopted a saddle-shaped conformation (Fig. 1b). The cavity diameters of **M₄** and **M₅** were determined to be approximately 6.5 and 8.5 Å, respectively. The curved conformations and defined cavities of **M₄** and **M₅** may make them ideal host candidates to recognize fullerenes (*vide infra*). All attempts to grow single crystals for hexamer **M₆** and heptamer **M₇** were unsuccessful. Therefore, a computational prediction of their conformations was performed at the RB3LYP/6-311G(d,p) level of theory. The calculated molecular geometries of hexamer **M₆** and heptamer **M₇** revealed that the macrocycles became further distorted with the increase of their size (Fig. S8 and S9†).

To evaluate the effect of *N*-alkyl and *N*-aryl substituents on the ionization potential of carbazole, the redox properties of **diBrCz-Ar** and **diBrCz-C4** were investigated by cyclic voltammetry (CV) in CH_2Cl_2 solution (potentials are referred vs. Fc/Fc^+) (Fig. S2†). The CV of **diBrCz-Ar** and **diBrCz-C4** exhibited one reversible oxidation wave with half-wave potentials of $E_{1/2} = +0.94$ V and $+1.10$ V, respectively. The ionization potential (IP) of **diBrCz-Ar** was estimated to be 5.26 eV, which was lower than that of **diBrCz-C4** (IP = 5.35 eV), indicating that the aryl substituent group could really reduce the ionization potential of carbazole (Table S1†). Interestingly, the CV of tetramer **M₄** showed four quasi-reversible oxidation waves (Fig. S3†), and its ionization potential (IP = 4.66 eV) was significantly decreased compared with that of **diBrCz-Ar** (Table S1†). The reversible voltammogram means that the radical states of **diBrCz-Ar** and tetramer **M₄** are most likely to be very stable, which directs us to investigate their radical cation species.

The synthesis of the stable carbazole radical cation is highly difficult arising from the relatively high oxidation potential of carbazole and the high reactivity/instability of the carbazole radical cation.^{3,4} For example, unlike triarylamine derivatives that can be readily oxidized by some common oxidants such as AgSbF_6 , SbCl_5 , $\text{Cu}(\text{ClO}_4)_2$ and so on, *N*-substituted carbazole compounds encounter the difficulty of effective one-electron oxidation under mild reaction conditions. Besides, most of the *N*-substituted carbazole compounds undergo the dimerization or polymerization reaction during the oxidation process, resulting in major difficulties in the isolation and precise structural characterization of the carbazole radical cation species.⁴ As a consequence, 2,3-dichloro-5,6-dicyano-1,4-benzoquinone (DDQ) was employed as an oxidant because of its strong electron-withdrawing ability. The solution of **diBrCz-Ar** immediately turned green after the addition of DDQ (Fig. 2a), implying the successful generation of the corresponding radical cation species (**diBrCz-Ar**⁺).^{4b} More specifically, the resultant green solution showed near-IR absorption beyond 1000 nm and this might suggest the formation of a singly charged primer, which was also observed in charged carbazole derivatives²⁰ and other π -systems.²¹ The electron paramagnetic resonance (EPR) spectrum of **diBrCz-Ar**⁺ provided direct evidence for the presence of the radical species (Fig. 2b, blue solid line). In comparison, tetramer **M**₄ could be oxidized by DDQ as well as AgSbF_6 due to its lower ionization potential (Fig. 2a), which is consistent with the voltammogram results. The EPR spectrum of **M**₄⁺ exhibited a strong single line in CH_2Cl_2 at room temperature (Fig. 2a, red solid line), implying efficient spin delocalization throughout the conjugated macrocycle. Notably, the radical cation species of **diBrCz-Ar**⁺ and **M**₄⁺ were extremely stable, as evidenced by their almost unchanged UV-vis absorption spectra for up to one week (Fig. 2c, S4 and S5†). In contrast, the *N*-alkyl substituted analogue **diBrCz-C4** could only be oxidized by DDQ in the presence of a strong acid (*e.g.*, methanesulfonic acid).^{4b} Moreover, the resultant radical cation species was very reactive, making it nearly impossible to purify and isolate **diBrCz-C4**⁺. The calculation results indicated that the spin density of the

carbazole radical can be delocalized on the aryl group as well as the whole macrocycle, which might account for the enhanced stability of the radical cation species of **diBrCz-Ar**⁺ and **M**₄⁺ (Fig. S10 and S11†).

Fortunately, single crystals of the carbazole radical cation species suitable for X-ray crystallographic analysis were successfully obtained by slow evaporation of the dichloromethane solution (Fig. 3). Interestingly, crystal structure analysis revealed a chemical moiety with a formula of $(\text{diBrCz-Ar})_2(\text{DDQ})$. Two **diBrCz-Ar** molecules were associated into inversion-centred dyads, which further alternated with one DDQ molecule into a one-dimensional (1D) chain along the *b*-axis, wherein face-to-face packing was observed in the dimerized **diBrCz-Ar** (Fig. 3a). In contrast, the packing motif of the neutral **diBrCz-Ar** was different from those of $(\text{diBrCz-Ar})_2(\text{DDQ})$ and two **diBrCz-Ar** molecules stacked in an offset fashion (Fig. 3b). The large bond length alternation found in the aromatic ring of DDQ suggested a mixed-valence state in $(\text{diBrCz-Ar})_2^{2+}(\text{DDQ})^{2-}$ rather than a full charge-transfer in $(\text{diBrCz-Ar})_2^{2+}(\text{DDQ})^{2-}$ (Fig. S24†).²² Thus, the carbazole radical cation species generated herein could be regarded as a mixed-valence radical cation of $(\text{diBrCz-Ar})_2^{2+}$. To the best of

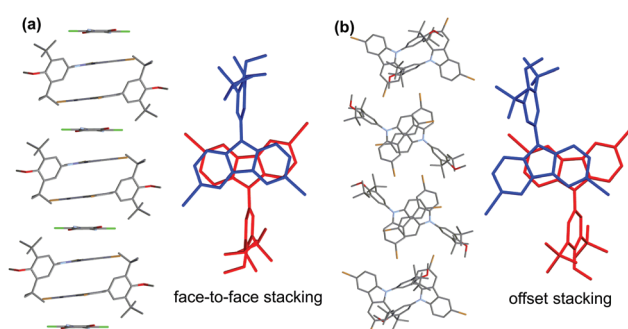


Fig. 3 The crystal structures and packing motifs of $(\text{diBrCz-Ar})_2(\text{DDQ})$ (a) and **diBrCz-Ar** (b). Hydrogen atoms and the solvent are omitted for clarity.

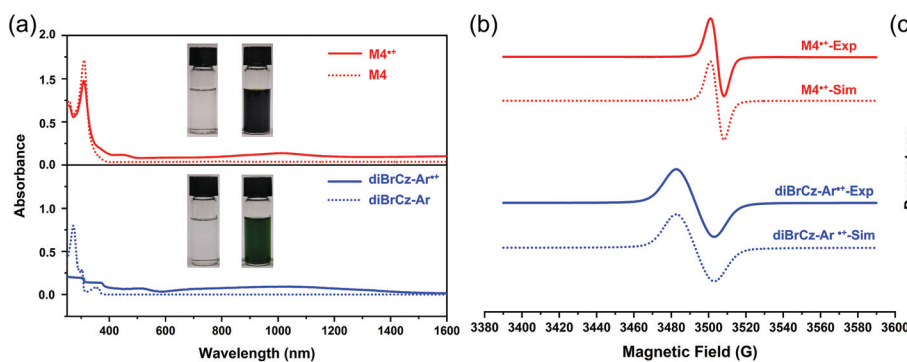


Fig. 2 (a) UV-vis-NIR spectra of **diBrCz-Ar** (blue line, bottom) and **M**₄ (red line, top) before (dashed line) and after (solid line) oxidation. The insets show the photographs of the solutions of neutral and oxidized **diBrCz-Ar** (bottom) and **M**₄ (top). (b) EPR spectra and simulations of **diBrCz-Ar**⁺ (blue line, bottom) and **M**₄⁺ (red line, top). (c) Evaluation of the stability of the radical cation species of **diBrCz-Ar**⁺ (blue column) and **M**₄⁺ (red column) using UV-vis-NIR spectroscopy.

our knowledge, this is the first time that a quality crystal of the carbazole radical cation was presented.³ All attempts to grow single crystals for radical cation \mathbf{M}_4^{+*} were unsuccessful. Thus, the structure of \mathbf{M}_4^{+*} was simulated at the UB3LYP/6-311G(d,p) level of theory (Fig. S11b†), wherein the spin density was fully delocalized over the whole molecule (Fig. S11c†).

Since tetramer \mathbf{M}_4 and pentamer \mathbf{M}_5 were relatively electron rich and possessed the distinct curved conformations and defined cavities, we speculated that they may serve as macrocyclic receptors towards fullerene recognition. The host–guest interactions between the macrocycles and fullerenes C_{60} and C_{70} were first examined by NMR spectroscopy. The ^1H NMR spectrum of \mathbf{M}_4 remained unchanged when mixed with fullerene C_{60} or C_{70} , implying negligible host–guest interactions between \mathbf{M}_4 and the fullerenes (Fig. 4a). Indeed, the cavity diameter (~ 6.5 Å) of \mathbf{M}_4 did not match well with the size of the fullerenes (~ 7.1 Å), and thus, it was too small to associate with them. In contrast, the addition of C_{60} or C_{70} to a solution of pentamer \mathbf{M}_5 in toluene- d_8 resulted in an obvious downfield shift of proton H^1 and slight upfield shifts of protons H^2 , H^3 ,

and H^4 of \mathbf{M}_5 (Fig. 4b), illustrating their considerable host–guest interactions. The observed set of NMR peaks suggested that the host–guest complexation between \mathbf{M}_5 and the fullerenes was a fast-exchange process within the NMR timescale at 298 K.^{9†} Moreover, the significant downfield shift of the inner proton H^1 was likely to indicate that the fullerenes might be encapsulated within the curved surface of \mathbf{M}_5 . In addition, the fluorescence intensity of \mathbf{M}_5 was quenched constantly with increasing concentration of C_{60} and C_{70} (Fig. 4c and d), further indicating their distinct host–guest interactions. To determine the binding stoichiometry of \mathbf{M}_5 and the fullerenes, the titration data were firstly obtained using the nonlinear regression models. The data were fitted to the association equilibria corresponding to the formation of inclusion complexes of 1:1 and 2:1 stoichiometries and a mixture of the two, respectively. Only the 1:1 model met the data, which indicated the presence of a 1:1 complex. Subsequently, Job plot analysis and MALDI-TOF MS also revealed a 1:1 stoichiometry of the complexation of \mathbf{M}_5 and the fullerenes (Fig. S18 and S19†). Fluorescence titration experiments in toluene solution also provided the association constants of $(8.38 \pm 0.33) \times 10^4 \text{ M}^{-1}$ and $(7.64 \pm 0.26) \times 10^4 \text{ M}^{-1}$ for $\mathbf{M}_5 \supset \text{C}_{60}$ and $\mathbf{M}_5 \supset \text{C}_{70}$, respectively, by fitting the concentration-dependent change of the emission intensity of \mathbf{M}_5 . The moderate association constants unambiguously demonstrated the existence of the host–guest interactions between \mathbf{M}_5 and the fullerenes. Furthermore, the additional peak observed in the UV-vis spectrum of the mixture of \mathbf{M}_5 and C_{60} revealed the intriguing charge transfer interactions between the electron-rich \mathbf{M}_5 and the electron-deficient fullerene (Fig. S17†). To gain insight into the structural information of the host–guest complex and their host–guest interaction, molecular mechanics simulations at the RB3LYP-D3/6-311+G(d,p) level of theory were also performed. The simulated structures of the host–guest complexes $\mathbf{M}_5 \supset \text{C}_{60}$ and $\mathbf{M}_5 \supset \text{C}_{70}$ revealed that the fullerenes fitted perfectly inside the concave cavity of \mathbf{M}_5 through multiple π – π interactions (Fig. 4e and f). Therefore, the above results indicate that both the electron-rich nature of \mathbf{M}_5 and its distinct curved conformation play a key role in fullerene recognition.

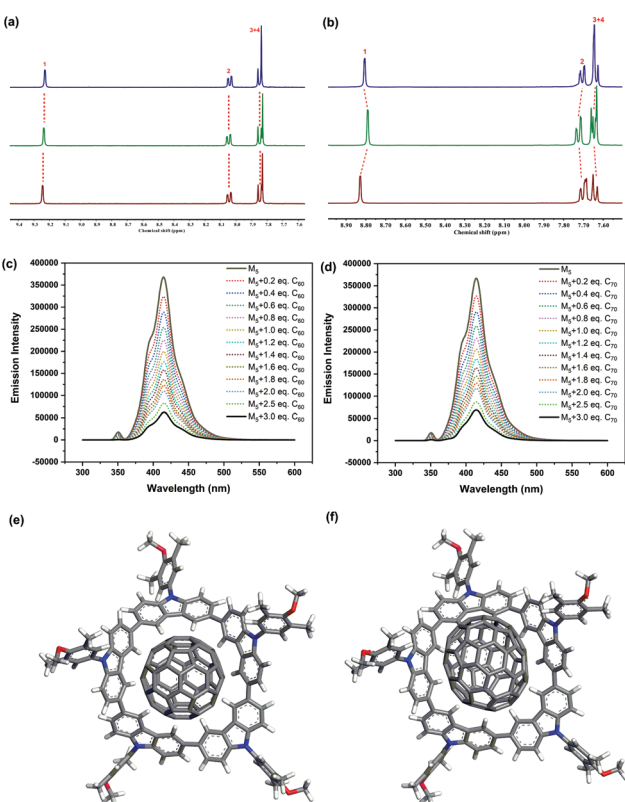


Fig. 4 (a) Partial ^1H NMR spectra (400 MHz, toluene- d_8 , 298 K) of solutions of 2.0 mM \mathbf{M}_4 + 2.0 mM C_{70} (top), 2.0 mM \mathbf{M}_4 (middle), and 2.0 mM \mathbf{M}_4 + 2.0 mM C_{60} (bottom). (b) Partial ^1H NMR spectra (400 MHz, toluene- d_8 , 298 K) of solutions of 2.0 mM \mathbf{M}_5 + 2.0 mM C_{70} (top), 2.0 mM \mathbf{M}_5 (middle), and 2.0 mM \mathbf{M}_5 + 2.0 mM C_{60} (bottom). (c) Complexation process of \mathbf{M}_5 and C_{60} . (d) Complexation process of \mathbf{M}_5 and C_{70} . (e) Top view of the optimized geometry of $\mathbf{M}_5 \supset \text{C}_{60}$ at the RB3LYP-D3/6-311+G(d,p) level of theory. (f) Top view of the optimized geometry of $\mathbf{M}_5 \supset \text{C}_{70}$ at the RB3LYP-D3/6-311+G(d,p) level of theory.

Conclusions

In summary, we have successfully synthesized a series of fully conjugated aryl carbazole-based macrocycles \mathbf{M}_n ($n = 4\text{--}7$) bearing a 3,5-di-*tert*-butyl-4-methoxyphenyl substituent. The bulky aryl group not only improved the solubility of the macrocycles but also reduced the ionization potential of the carbazole building block as well as the macrocycles. As a consequence, the aryl carbazole and \mathbf{M}_4 were readily oxidized into radical cation species in the presence of DDQ. The resultant radical cation species were found to be very stable because the spin density can be delocalized on the aryl group as well as the whole macrocycle. Notably, a mixed-valence radical cation of $(\text{diBrCz-Ar})_2^{+*}$ was successfully isolated and confirmed by X-ray crystallography. Moreover, pentamer \mathbf{M}_5 possessed a curved

conformation and defined cavity, making it an ideal macrocyclic host candidate to recognize fullerenes. The excellent fullerene recognition ability of **M**₅ was also attributed to the electron-rich nature of aryl carbazole, leading to the obvious charge transfer interactions between **M**₅ and C₆₀. The aryl-functionalization strategy in this study will shed some light on the design of novel macrocyclic arenes, which may exhibit some distinct properties compared with their alkyl substituted analogues.

Conflicts of interest

There are no conflicts to declare.

Acknowledgements

X. S. acknowledges the financial support sponsored by the NSFC, China (No. 22071061 and 52003081), the Shanghai Sailing Program (19YF1412900) and the Microscale Magnetic Resonance Platform of ECNU.

References

- (a) J. V. Grazulevicius, P. Strohriegl, J. Pielichowski and K. Pielichowskic, Carbazole-containing polymers: synthesis, properties and applications, *Prog. Polym. Sci.*, 2003, **28**, 1297–1353; (b) K. Ivaniuk, V. Cherpak, P. Stakhira, Z. Hotra, B. Minaev, G. Baryshnikov, E. Stromylo, D. Volyniuk, J. V. Grazulevicius, A. Lazauskas, S. Tamulevicius, B. Witulski, M. E. Light, P. Gawrys, R. J. Whitby, G. Wiosna-Salyga and B. Luszczynska, Highly luminous sky-blue organic light-emitting diodes based on the bis[(1,2)(5,6)]indoloanthracene emissive layer, *J. Phys. Chem. C*, 2016, **120**, 6206–6217; (c) Z. Zeng, X. Shi, C. Chi, J. T. L. Navarrete, J. Casado and J. Wu, Pro-aromatic and anti-aromatic π -conjugated molecules: an irresistible wish to be diradicals, *Chem. Soc. Rev.*, 2015, **44**, 6578–6596.
- (a) F. Dumur, Carbazole-based polymers as hosts for solution-processed organic light-emitting diodes: Simplicity, efficacy, *Org. Electron.*, 2015, **25**, 345–361; (b) B. Wex and B. R. Kaafarani, Perspective on carbazole-based organic compounds as emitters and hosts in TADF applications, *J. Mater. Chem. C*, 2017, **5**, 8622–8653.
- (a) Y. Tsuji, A. Tsuchida, Y. Onogi and M. Yamamoto, Stabilization of carbazole radical cation formed in poly (N-vinylcarbazole) by charge delocalization, *Macromolecules*, 1990, **23**, 4019–4023; (b) L. Fajári, R. Papoula, M. Reig, E. Brillas, J. Jordà, O. Vallcorba, J. Rius, D. Velasco and L. Juliá, Charge transfer states in stable neutral and oxidized radical adducts from carbazole derivatives, *J. Org. Chem.*, 2014, **79**, 1771–1777; (c) S. Kasemthaveechok, L. Abella, M. Jean, M. Cordier, T. Roisnel, N. Vanthuyne, T. Guizouarn, O. Cador, J. Autschbach, J. Crassous and L. Favereau, Axially and helically chiral cationic radical bicarbazoles: SOMO–HOMO level inversion and chirality impact on the stability of mono- and diradical cations, *J. Am. Chem. Soc.*, 2020, **142**, 20409–20418.
- (a) K. Karon and M. Lapkowski, Carbazole electrochemistry: a short review, *J. Solid State Electrochem.*, 2015, **19**, 2601–2610; (b) S. Mallick, S. Maddala, K. Kollimalayan and P. Venkatakrishnan, Oxidative coupling of carbazoles: a substituent-governed regioselectivity profile, *J. Org. Chem.*, 2019, **84**, 73–93.
- (a) N. Morohashi, F. Narumi, N. Iki, T. Hattori and S. Miyano, Thiocalixarenes, *Chem. Rev.*, 2006, **106**, 5291–5316; (b) M.-X. Wang, Nitrogen and oxygen bridged calixaromatics: synthesis, structure, functionalization, and molecular recognition, *Acc. Chem. Res.*, 2012, **45**, 182–195; (c) Y. Zhou, H. Li and Y.-W. Yang, Controlled drug delivery systems based on calixarenes, *Chin. Chem. Lett.*, 2015, **26**, 825–828; (d) J.-M. Yang, Y. Yu and J. Rebek Jr., Selective macrocycle formation in cavitands, *J. Am. Chem. Soc.*, 2021, **143**, 2190–2193.
- (a) M. Ciardi, F. Tancini, G. Gil-Ramírez, E. C. E. Adán, C. Massera, E. Dalcanale and P. Ballester, Switching from separated to contact ion-pair binding modes with diastereomeric calix[4]pyrrole bis-phosphonate receptors, *J. Am. Chem. Soc.*, 2012, **134**, 13121–13132; (b) S. K. Kim and J. L. Sessler, Calix[4]pyrrole-based ion pair receptors, *Acc. Chem. Res.*, 2014, **47**, 2525–2536.
- (a) J. W. Lee, S. Samal, N. Selvapalam, H.-J. Kim and K. Kim, Cucurbituril homologues and derivatives: new opportunities in supramolecular chemistry, *Acc. Chem. Res.*, 2003, **36**, 621–630; (b) S. J. Barrow, S. Kasera, M. J. Rowland, J. D. Barrio and O. A. Scherman, Cucurbituril-based molecular recognition, *Chem. Rev.*, 2015, **115**, 12320–12406; (c) Y. Dong and L. Cao, Functionalization of Cucurbit uril, *Prog. Chem.*, 2016, **28**, 1039–1053.
- (a) T. Ogoshi, S. Kanai, S. Fujinami, T.-A. Yamagishi and Y. Nakamoto, Para-bridged symmetrical pillar[5]arenes: their Lewis acid catalyzed synthesis and host-guest property, *J. Am. Chem. Soc.*, 2008, **130**, 5022–5023; (b) D. Cao, Y. Kou, J. Liang, Z. Chen, L. Wang and H. Meier, A facile and efficient preparation of pillararenes and a pillarquinoine, *Angew. Chem., Int. Ed.*, 2009, **48**, 9721–9723; (c) M. Xue, Y. Yang, X. Chi, Z. Zhang and F. Huang, Pillararenes, a new class of macrocycles for supramolecular chemistry, *Acc. Chem. Res.*, 2012, **45**, 1294–1308; (d) T. Ogoshi, T.-A. Yamagishi and Y. Nakamoto, Pillararenes, a new class of macrocycles for supramolecular chemistry, *Chem. Rev.*, 2016, **116**, 7937–8002.
- (a) R. Jasti, J. Bhattacharjee, J. B. Neaton and C. R. Bertozzi, Synthesis, characterization, and theory of [9]–[12]–, and [18] cycloparaphenylenes: carbon nanohoop structures, *J. Am. Chem. Soc.*, 2008, **130**, 17646–17647; (b) A. Ito, Y. Yokoyama, R. Aihara, K. Fukui, S. Eguchi, K. Shizu, T. Sato and K. Tanaka, Preparation and Characterization of N-Anisyl-Substituted Hexaaza[16]paracyclophane, *Angew. Chem., Int. Ed.*, 2010, **49**, 8205–8208; (c) W. Si, Z.-T. Li and

J.-L. Hou, Voltage-driven reversible insertion into and leaving from a lipid bilayer: Tuning transmembrane transport of artificial channels, *Angew. Chem., Int. Ed.*, 2014, **53**, 4578–4581; (d) H. Chen, J. Fan, X. Hu, J. Ma, S. Wang, J. Li, Y. Yu, X. Jia and C. Li, Biphen[n]arenes, *Chem. Sci.*, 2015, **6**, 197–202; (e) Y. Zhou, H.-Y. Zhang, Z.-Y. Zhang and Y. Liu, Tunable luminescent lanthanide supramolecular assembly based on photoreaction of anthracene, *J. Am. Chem. Soc.*, 2017, **139**, 7168–7171; (f) Y. Yang, P. He, Y. Wang, H. Bai, S. Wang, J.-F. Xu and X. Zhang, Supramolecular radical anions triggered by bacteria *in situ* for selective photothermal therapy, *Angew. Chem., Int. Ed.*, 2017, **56**, 16239–16242; (g) L. Mao, W. Pan, Y. Fu, L. Chen, M. Xu, Y. Ren, W. Feng and L. Yuan, Reversibly tunable lower critical solution temperature behavior induced by H-bonded aromatic amide macrocycle and imidazolium host-guest complexation, *Org. Lett.*, 2017, **19**, 18–21; (h) S. Guo, Y. Song, Y. He, X.-Y. Hu and L. Wang, Highly efficient artificial light-harvesting systems constructed in aqueous solution based on supramolecular self-assembly, *Angew. Chem., Int. Ed.*, 2018, **57**, 3163–3167; (i) W. Wang, C. Chen, C. Shu, S. Rajca, X. Wang and A. Rajca, S = 1 Tetraazacyclophane diradical dication with robust stability: a case of low-temperature one-dimensional antiferromagnetic chain, *J. Am. Chem. Soc.*, 2018, **140**, 7820–7826; (j) H. Ke, L.-P. Yang, M. Xie, Z. Chen, H. Yao and W. Jiang, Shear-induced assembly of a transient yet highly stretchable hydrogel based on pseudo-polyrotaxanes, *Nat. Chem.*, 2019, **11**, 470–477; (k) L. Mao, Y. Hu, Q. Tu, W.-L. Jiang, X.-L. Zhao, W. Wang, D. Yuan, J. Wen and X. Shi, Highly efficient synthesis of non-planar macrocycles possessing intriguing self-assembling behaviors and ethene/ethyne capture properties, *Nat. Commun.*, 2020, **11**, 5806; (l) J.-Q. Wang, Y. Han and C.-F. Chen, 3,6-Fluoren[5]arenes: synthesis, structure and complexation with fullerenes C₆₀ and C₇₀, *Chem. Commun.*, 2021, **57**, 3987–3990; (m) Y. Wang, H. Wu and J. F. Stoddart, Molecular triangles: a new class of macrocycles, *Acc. Chem. Res.*, 2021, **54**, 2027–2039; (n) X. Lu, T. Y. Gopalakrishna, Y. Han, Y. Ni, Y. Zou and J. Wu, Bowl-shaped carbon nanobelts showing size-dependent properties and selective encapsulation of C₇₀, *J. Am. Chem. Soc.*, 2019, **141**, 5934–5941.

10 J. R. Dobscha, H. D. Castillo, Y. Li, R. E. Fadler, R. D. Taylor, A. A. Brown, C. Q. Trainor, S. L. Tait and A. H. Flood, Sequence-defined macrocycles for understanding and controlling the build-up of hierarchical order in self-assembled 2D arrays, *J. Am. Chem. Soc.*, 2019, **141**, 17588–17600.

11 S.-i. Kawano, Y. Ishida and K. Tanaka, Columnar liquid-crystalline metallomacrocycles, *J. Am. Chem. Soc.*, 2015, **137**, 2295–2302.

12 (a) K. Tani, Y. Tohda, H. Takemura, H. Ohkita, S. Itoc and M. Yamamoto, Synthesis and photophysical properties of [3.3](3, 9) carbazolophanes, *Chem. Commun.*, 2001, 1914–1915; (b) N. Sharma, E. Spulung, C. M. Mattern, W. Li, O. Fuhr, Y. Tsuchiya, C. Adachi, S. Bräse, I. D. W. Samuel and E. Zysman-Colman, Turn on of sky-blue thermally activated delayed fluorescence and circularly polarized luminescence (CPL) via increased torsion by a bulky carbazolophane donor, *Chem. Sci.*, 2019, **10**, 6689–6696.

13 P. Yang, Y. Jian, X. Zhou, G. Li, T. Deng, H. Shen, Z. Yang and Z. Tian, Calix[3]carbazole: one-step synthesis and host-guest binding, *J. Org. Chem.*, 2016, **81**, 2974–2980.

14 (a) D. Myśliwiec, M. Kondratowicz, T. Lis, P. J. Chmielewski and M. Stępień, Highly strained nonclassical nanotube end-caps. A single-step solution synthesis from strain-free, non-macrocyclic precursors, *J. Am. Chem. Soc.*, 2015, **137**, 1643–1649; (b) F. Lucas, L. Sicard, O. Jeannin, J. Rault-Berthelot, E. Jacques, C. Quinton and C. Porié, [4]Cyclo-N-ethyl-2,7-carbazole synthesis, structural, electronic and charge transport properties, *Chem. – Eur. J.*, 2019, **25**, 7740–7748; (c) Y. Kuroda, Y. Sakamoto, T. Suzuki, E. Kayahara and S. Yamago, Tetracyclo(2,7-carbazole)s: diatropicity and paratropicity of inner regions of nanohoops, *J. Org. Chem.*, 2016, **81**, 3356–3363; (d) K. Senthilkumar, M. Kondratowicz, T. Lis, P. J. Chmielewski, J. Cybińska, J. Zafra, J. Casado, T. Vives, J. Crassous, L. Favereau and M. Stępień, Lemniscular [16]cycloparaphenylenes: a radially conjugated figure-eight aromatic molecule, *J. Am. Chem. Soc.*, 2019, **141**, 7421–7427; (e) M. Hermann, D. Wassy and B. Esser, Conjugated nanohoops incorporating donor, acceptor, hetero- or polycyclic aromatics, *Angew. Chem., Int. Ed.*, 2021, DOI: 10.1002/anie.202007024.

15 (a) J. Ostrauskaite and P. Strohriegel, Formation of macrocycles in the synthesis of poly(N-(2-ethylhexyl)carbazol-3,6-diyl), *Macromol. Chem. Phys.*, 2003, **204**, 1713–1718; (b) L. S. Coumont and J. G. C. Veinot, Ni(COD)₂ coupling of 3, 6-dibromocarbazoles as a route to all-carbazole shape persistent macrocycles, *Tetrahedron Lett.*, 2015, **56**, 5595–5598; (c) H. Zhu, B. Shi, K. Chen, P. Wei, D. Xia, J. H. Mondal and F. Huang, Cyclo[4]carbazole, an iodide anion macrocyclic receptor, *Org. Lett.*, 2016, **18**, 5054–5057; (d) H. Zhu, I. Badía-Domínguez, B. Shi, Q. Li, P. Wei, H. Xing, M. C. R. Delgado and F. Huang, Cyclization-promoted ultralong low-temperature phosphorescence via boosting intersystem crossing, *J. Am. Chem. Soc.*, 2021, **143**, 2164–2169.

16 K. Balakrishnan, A. Datar, W. Zhang, X. Yang, T. Naddo, J. Huang, J. Zuo, M. Yen, J. S. Moore and L. Zang, Nanofibril self-assembly of an arylene ethynylene macrocycle, *J. Am. Chem. Soc.*, 2006, **128**, 6576–6577.

17 H. Xu, F.-J. Qian, Q.-X. Wu, M. Xue, Y. Yang and Y.-X. Chen, Azacalix[2]arene[2]carbazoles: synthesis, structure and properties, *RSC Adv.*, 2016, **6**, 27988–27992.

18 S. Shanmugaraju, V. Vajpayee, S. Lee, K.-W. Chi, P. J. Stang and P. S. Mukherjee, Coordination-driven self-assembly of 2D-metallamacrocycles using a new carbazole-based dipyridyl donor: synthesis, characterization, and C₆₀ binding study, *Inorg. Chem.*, 2012, **51**, 4817–4823.

19 (a) A. Rüütel, V. Yrjänä, S. A. Kadam, I. Saar, M. Ilisson, A. Darnell, K. Haav, T. Haljasorg, L. Toom, J. Bobacka and I. Leito, Design, synthesis and application of carbazole

macrocycles in anion sensors, *Beilstein J. Org. Chem.*, 2020, **16**, 1901–1914; (b) D. Myśliwiec, T. Lis, J. Gregoliński and M. Stępień, Stereoselective Wittig Olefination as a macrocyclization tool. synthesis of large carbazolophanes, *J. Org. Chem.*, 2015, **80**, 6300–6312.

20 (a) T. Suzuki, W. Nojo, Y. Sakano, R. Katoono, Y. Ishigaki, H. Ohno and K. Fujiwara, Redox-induced conformational changes in 1,3-propylene- and m-xylylenebis[5-(10-butyl-5,10-dihydrobenzo[a]indolo[2,3-c]carbazole)]: twin-BIC donors that form sandwich-like dimeric cations exhibiting NIR absorption, *Chem. Lett.*, 2016, **45**, 720–722; (b) W. Nojo, Y. Ishigaki, T. Takeda, T. Akutagawa and T. Suzuki, Selective formation of a mixed-valence state from linearly bridged oligo(aromatic diamines): drastic structural change into a folded columnar stack for half-filled polycations, *Chem. – Eur. J.*, 2019, **25**, 7759–7765.

21 (a) L. Ballester, A. Gutieérrez, M. F. Perpñán and S. Rico, Magnetic behavior and crystal structure of [Fe(cyclam)(NCS)₂](TCNQ)₂: an unusual one-dimensional (TCNQ)₂-radical-ion system, *Inorg. Chem.*, 1999, **38**, 4430–4434; (b) V. Ganesan, S. V. Rosokha and J. K. Kochi, Isolation of the latent precursor complex in electron-transfer dynamics. Intermolecular association and self-exchange with acceptor anion radicals, *J. Am. Chem. Soc.*, 2003, **125**, 2559–2571; (c) J.-M. Lü, S. V. Rosokha and J. K. Kochi, Stable (long-bonded) dimers via the quantitative self-association of different cationic, anionic, and uncharged π -radicals: structures, energetics, and optical transitions, *J. Am. Chem. Soc.*, 2003, **125**, 12161–12171.

22 J. S. Miller and D. A. Dixon, Dianion stabilization by $(M(C_5(CH_3)_5)_2)^+$: theoretical evidence for a localized ring in (DDQ)₂[–], *Science*, 1987, **235**, 871–873.